Analyst

PAPER

View Article Online
View Journal

Cite this: DOI: 10.1039/c6an00018e

An oligonucleotide-functionalized carbon nanotube chemiresistor for sensitive detection of mercury in saliva†

Dawit N. Wordofa,‡[a] Pankaj Ramnani,‡[a] Thien-Toan Tran[b] and Ashok Mulchandani*[a,c]

Received 4th January 2016,
Accepted 15th February 2016

DOI: 10.1039/c6an00018e

www.rsc.org/analyst

Divalent mercuric (Hg^{2+}) ion and monomethyl mercury (CH_3Hg^+) are two forms of mercury that are known to be highly toxic to humans. In this work, we present a highly selective, sensitive and label-free chemiresistive biosensor for the detection of both, Hg^{2+} and CH_3Hg^+ ions using DNA-functionalized single-walled carbon nanotubes (SWNTs). The SWNTs were functionalized with the capture oligonucleotide, polyT, using a linker molecule. The polyT was hybridized with polyA to form a polyT:polyA duplex. Upon exposure to mercury ions, the polyT:polyA duplex dehybridizes and a T–Hg^{2+}–T duplex is formed. This structure switch leads to the release of polyA from the SWNT surface and correspondingly a change in the resistance of the chemiresistive biosensor is observed, which is used to quantify the mercury ion concentration. The biosensor showed a wide dynamic range of 0.5 to 100 nM for the detection of CH_3Hg^+ ions in buffer solution with a sensitivity of 28.34% per log (nM) of CH_3Hg^+. Finally, real world application of the biosensor was demonstrated by the detection of Hg^{2+} and CH_3Hg^+ ions in simulated saliva samples spiked with a known concentration of mercury ions.

Introduction

Mercury (Hg) is a toxic metal-pollutant in the environment that can exist in elemental, inorganic and/or organic forms and each form is known to have a distinct toxicity profile.[1] While the inorganic form of mercury ($HgCl_2$) is toxic to kidneys,[2] organic forms such as methylmercury are primarily neurotoxins that affect the central nervous system.[3] Methylmercury is also known to have genotoxic effects and fetal exposure can cause intrauterine poisoning at lower exposure levels.[4] Methylmercury has a strong affinity to amino acids and eventually binds to proteins and polypeptide chains.[5] Humans are exposed to different forms of mercury due to natural causes such as off-gassing from the earth's crust and anthropogenic sources such as environmental pollution caused by industrial utilization and the use of pesticides in agricultural practices.[6] Mercury is methylated by the microorganisms present in water and bioconcentrated *via* the aquatic food chain.[7] This eventually results in human exposure due to the consumption of fish and contaminated water. Incidents of epidemic outbreaks due to mercury poisoning have been reported in the past. In the mid-1950s, waste containing methylmercury was discharged into the Minamata Bay in Japan by Chisso Corporation, a large acetaldehyde producing factory, leading to bioaccumulation of the toxic chemical in the shellfish and fish. When these fish were consumed by the local population, it resulted in large scale mercury poisoning among the residents of Minamata Bay in Japan.[8] In 1972, a similar incident of mass poisoning by methylmercury was reported in Iraq due to direct contamination of food from the use of pesticides containing methylmercury in agriculture.[9] As a consequence, about 6500 patients were hospitalized and nearly 460 people died. Recent studies demonstrate that there is still a concern of exposure to methylmercury and elemental mercury from industrial activities. Silver/gold-mercury amalgam dental fillings are another potential source of mercury exposure receiving scrutiny.[10] It is hypothesized that Hg^0 vapors emitted from amalgams are first converted to Hg^{2+} and then transformed to CH_3Hg^+ by oral bacteria.[11] Hence, the detection of mercury in several matrices including human saliva is an indispensable task.[12]

The commonly used techniques used for mercury detection include cold-vapor atomic absorption spectroscopy,[13] atomic

[a]Department of Chemical and Environmental Engineering, University of California, Riverside, California 92521, USA. E-mail: adani@engr.ucr.edu; Tel: +1-951-827-6419
[b]Department of Bioengineering, University of California, Riverside, California 92521, USA
[c]Material Science and Engineering Program, University of California, Riverside, California 92521, USA

†Electronic supplementary information (ESI) available. See DOI: 10.1039/c6an00018e

‡These authors contributed equally.

fluorescence spectrometry,[14] and inductively coupled plasma spectrometry.[15] These techniques though highly sensitive and reliable have certain limitations such as complex sample preparation, use of expensive instruments, need for well-trained technicians and longer assay times. Hence, it is very important to develop a highly selective, sensitive, rapid and cost effective sensor for the detection of mercury.

To address these issues, electrochemical biosensors that incorporate a variety of bioreceptors and transducers for the detection of heavy metals have been discussed in the literature.[16,17] In particular, electrochemical biosensors based on carbon nanotubes as the transducer element have been widely used for effective, rapid and robust analysis of environmental samples.[18,19] Owing to their high surface area to volume ratio, the electrical properties of carbon nanotubes are highly sensitive to any surface perturbations or binding events and enable label-free detection of analytes. Gong *et al.*[20] reported a DNA-based SWNT biosensor for label-free, selective and highly sensitive detection of Hg^{2+} using a polyT:polyA duplex functionalized SWNT. In this paper we use a similar detection scheme for the detection of both Hg^{2+} and CH_3Hg^+ in phosphate buffer and simulated saliva. A detailed detection scheme is shown in Fig. 1. Briefly, the SWNTs are functionalized with the capture oligonucleotide polyT, which hybridizes with polyA to form a DNA duplex. Upon exposure to mercury (Hg^{2+} and CH_3Hg^+), a structure switch occurs as the polyT:polyA duplex dehybridizes to form a T–Hg^{2+}–T complex[21,22] and polyA is released from the SWNT surface. These events lead to a change in the resistance of the chemiresistive biosensor which is used to quantify the concentration of mercury. We demonstrate the real world application of the proposed biosensor by evaluating the performance against mercury ions spiked in simulated human saliva samples. The present work is original and significantly different from the previous publication[20] of Hg^{2+} detection by using a structure switching DNA based chemiresistor biosensor in the following respects. (1) This is the first demonstration of methyl mercury (CH_3Hg^+) detection by using a structure-switching polyT:polyA DNA duplex recognition element. (2) It is the first report of label-free electronic detection of CH_3Hg^+ by a chemiresistor biosensor. (3) This is the first time a SWNT chemiresistor/electronic biosensor is applied for the detection of mercury in biological samples. (4) It uses a new protocol for preparing a SWNT network chemiresistor transducer device based on 3-Aminopropyltriethoxysilane (APTES)-directed self-assembly of 95% semi-conducting SWNTs instead of AC dielectrophoretic driven network formation of 66% semi-conducting SWNTs, producing a much denser and uniform network of carbon nanotubes and consequently a higher sensitivity.

Experimental section

Materials and apparatus

All the chemicals used in this study were reagent grade and purchased from Fisher Scientific unless stated otherwise. Mercuric chloride ($HgCl_2$) crystals (99.5%) were used to prepare different concentrations of Hg^{2+} solution samples. Monomethyl mercury (CH_3Hg^+) stock solution was prepared by dissolving a desired mass of methylmercury-chloride (CH_3HgCl) (Crescent Chemical; >96%) in deionized water. Single-walled carbon nanotube (SWNT) solution (0.01 mg ml^{-1}, 95% semiconducting) was purchased from NanoIntegris Inc. PolyT (5′-TTT TTT TTT TTT TTT-3′) and polyA (5′-AAA AAA AAA AAA AAA-3′) oligonucleotides were purchased from Integrated DNA Technologies Inc. (IDT). Blocking reagents, including

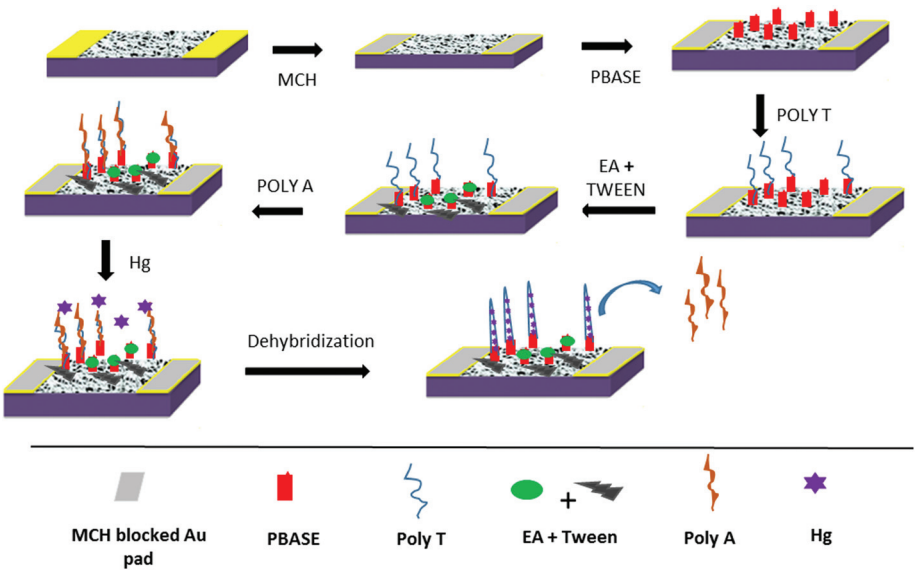

Fig. 1 Schematic illustration of SWNT chemiresistive label-free biosensor surface functionalization and detection.

6-mercapto-1-hexanol (MCH, 97%), ethanolamine (EA, 99%) and Tween 20 were purchased from Sigma Aldrich, Acros Organics and Bio-Rad respectively. 3-Aminopropyltriethoxysilane (APTES, 99%) was purchased from Acros Organics. 1-Pyrenebutanoic acid succinimidyl ester (PBASE) was purchased from Invitrogen Inc. A CHI660 electrochemical workstation was used to obtain the current–voltage (*I–V*) characteristics and a scanning electron microscope (Leo 1550) was used to examine the morphology of the SWNTs.

Simulated human saliva preparation

Simulated human saliva was prepared based on the composition reported previously.[23] The simulated saliva consisted of 0.6 g L^{-1} of sodium phosphate dibasic, 0.6 g L^{-1} of anhydrous calcium chloride, 0.4 g L^{-1} of potassium chloride, 0.4 g L^{-1} of sodium chloride, 4 g L^{-1} of mucin and 4 g L^{-1} of urea dissolved in DI water. The pH was adjusted to 7.2 and the solution was stored in the refrigerator until use.

Device fabrication and surface functionalization

The SWNT devices were fabricated using the protocol reported by Ramnani *et al.*[24] Briefly, the interdigitated electrodes fabricated using standard lithography were incubated with APTES to assist uniform and dense immobilization of SWNTs on the substrate. Subsequently, the APTES functionalized chips were incubated with 50 μL of SWNT solution (0.01 mg ml^{-1}) for 30 min, followed by annealing in air at 250 °C. To prevent any non-specific binding of proteins and mercury ions to the gold pads, the SWNT functionalized chips were incubated with 2 mM MCH solution prepared in dimethylformamide (DMF) for 30 min. Next, the SWNT network was non-covalently modified with the bilinker molecule, PBASE (6 mM solution prepared in DMF) through π–π bond formation between pyrene and SWNTs. The PBASE-modified SWNTs were incubated overnight with 100 nM of amine-labeled polyT (5′-/5AmMC6/TTT TTT TTT TTT TTT-3′) in phosphate buffer (PB, 10 mM, pH 7.4) at 4 °C. The oligonucleotide was immobilized covalently *via* an amide bond between the amine at the 5′ end and the ester groups of PBASE. The device was further treated with 0.1 mM EA to block excess ester groups and 0.1% Tween 20 to prevent non-specific binding to SWNTs. Finally, the polyT captured on the SWNT surface was hybridized with polyA (5′-AAA AAA AAA AAA AAA-3′) by incubating with 100 nM polyA in PB for 2 hours at room temperature to form a DNA duplex. The above fabrication and functionalization steps were monitored by recording the current–voltage (*I–V*) characteristics of the device between −0.1 and +0.1 V after each incubation step using a CHI660 electrochemical workstation.

Sensing protocol

SWNTs functionalized with the polyT:polyA duplex were incubated with increasing concentrations of Hg^{2+} and CH_3Hg^+ ion samples in PB for 30 min at room temperature. Following incubation, the chips were rinsed with PB three times to remove the unbound mercury ions and the resistance was measured by taking the inverse of the slope of the *I–V* curve from −0.1 V to +0.1 V under wet conditions, *i.e.* the sensing area covered with PB. A schematic of the device fabrication and sensing protocol is shown in Fig. 1.

For the detection of mercury in biological samples, simulated human saliva was spiked with different concentrations of Hg^{2+}/CH_3Hg^+ and incubated on DNA-duplex-functionalized SWNTs.

Results and discussion

The current–voltage (*I–V*) characteristics were recorded after each step of surface modification during fabrication and subsequently when exposed to CH_3Hg^+ in PB for sensing. As shown in Fig. 2(A), the resistance of the device increased following each treatment step, *i.e.* MCH, PBASE, polyT, EA, Tween 20 and polyA. The increase in resistance for the above steps is attributed to the change in the work function of gold due to the formation of Au–S bonds, π–π interaction between SWNTs and pyrene moieties in PBASE, electron donation from amine-labeled polyT, EA, Tween 20 and polyA resulting in a decrease of the charge carrier concentration of the p-type SWNTs and/or electron scattering from these molecules. In the final step, the DNA duplex functionalized devices were incubated with

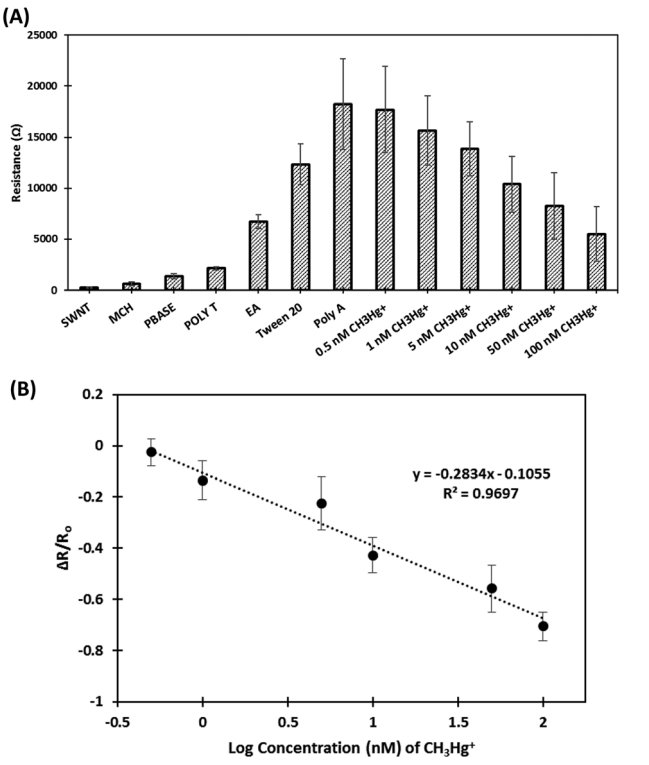

Fig. 2 (A) Change in resistance observed after each device functionalization step and upon exposure to CH_3Hg^+; (B) calibration curve for detection of CH_3Hg^+ in PB. Each data point is an average of measurements from 8 independent sensors and error bars represent ±1 standard deviation.

different concentrations of CH_3Hg^+ in PB solution (10 mM, pH 7.4). Similar to Hg^{2+} (Fig. S1†), upon incubation of the DNA duplex functionalized biosensor with increasing concentrations of CH_3Hg^+ a decrease in device resistance was observed. To verify that the change in resistance upon exposure to CH_3Hg^+ was specifically due to the displacement of polyA from the polyT:polyA duplex, a control experiment was performed where the response of the polyT-functionalized SWNTs was measured for increasing concentrations of CH_3Hg^+ in the absence of polyA. As shown in Fig. S2,† SWNTs functionalized with only the capture oligonucleotide (polyT) showed no significant changes in resistance upon incubation with CH_3Hg^+. Another control experiment was performed where the response of SWNTs to CH_3Hg^+ in the absence of polyT and polyA was measured. A negligible change in resistance with increasing CH_3Hg^+ concentrations (data not shown) confirmed the absence of any non-specific binding between SWNTs and CH_3Hg^+. These control experiments confirmed that the DNA duplex was primarily responsible for the nanobiosensor response to CH_3Hg^+. In a separate control experiment, the effectiveness of blocking of gold pads using 6-mercapto-1-hexanol (MCH) was evaluated. Without MCH treatment, the devices showed an increase in the device resistance upon exposure to CH_3Hg^+, which was attributed to CH_3Hg^+ binding to gold electrodes, changing the work function of gold. However, this non-specific binding was almost eliminated when the gold pads were blocked with MCH (Table S1†).[25] Similar to the mechanism in the case of Hg^{2+}, the decrease in the device resistance upon incubation with CH_3Hg^+ is hypothesized to be a result of dehybridization of the polyT:polyA duplex and subsequent release of polyA from the SWNT surface due to its binding to polyT and possibly the formation of a thymine–CH_3Hg^+–thymine duplex.

Fig. 2(B) shows the calibration curve, normalized change in resistance $[(R - R_o)/R_o$, where R is the resistance after incubation with CH_3Hg^+ and R_o is the resistance after hybridization between polyT and polyA] as a function of log concentration of CH_3Hg^+ (in nM). The sensor showed a linear response over the range of CH_3Hg^+ concentrations varying from 0.5 nM to 100 nM and a linear regression equation of $y = -0.2834x - 0.1055$ ($R^2 = 0.9697$) was obtained. The biosensor sensitivity for CH_3Hg^+ was slightly higher than that for Hg^{2+} (Fig. S1†). As shown in Fig. S1,† a linear response was observed for Hg^{2+} concentrations varying from 1 nM to 1000 nM and a linear regression equation of $y = -0.2164x - 0.2549$ ($R^2 = 0.9145$). Thus, the DNA-switching based biosensor responds to both mercury ions and would be suitable for measuring total mercury concentration but not for speciation of the mercury ion species. Further, the sensitivity achieved for Hg^{2+} was higher than that reported by Gong *et al.*[20] due to the improved device performance resulting from the use of high purity SWNTs (95% *vs.* 66%) and a denser network of SWNTs obtained through APTES-assisted assembly compared to the dielectrophoresis alignment method.

Detection of mercury in simulated saliva

As discussed earlier, the most common sources of mercury poisoning among humans is *via* consumption of fish that contain mercury and amalgam dental fillings. Detection of mercury in body fluids such as urine, saliva and/or blood can serve as a diagnostic tool for the early detection of health issues. Although analysis of urine samples is a universally accepted diagnostic tool to assess exposures to a broad range of toxic metals particular mercury, over the recent years there has been a growing interest in the detection of disease biomarkers/toxins in saliva due to the ease of sample collection in a noninvasive manner.[26] The use of SWNT chemiresistor-based biosensors for the detection of stress biomarkers in saliva (salivary α-amylase) has been reported by our group.[23] In this work, we evaluated the performance of our biosensor against simulated saliva samples spiked with mercury (both, Hg^{2+} and CH_3Hg^+) to demonstrate its practical application.

The DNA-functionalized SWNT biosensor was tested for the detection of mercury in simulated saliva samples spiked with varying concentrations of both Hg^{2+} and CH_3Hg^+. It is critical to note that mucins, a large group of glycoprotein molecules present in saliva, are known to non-specifically interact with nonpolar/hydrophobic surfaces. Since this non-specific adsorption is low on uncharged polar groups such as hydroxyl (–OH),[27] the blocking of gold pads using 6-mercapto-1-hexanol (MCH) makes the surface hydrophilic and alleviates the non-

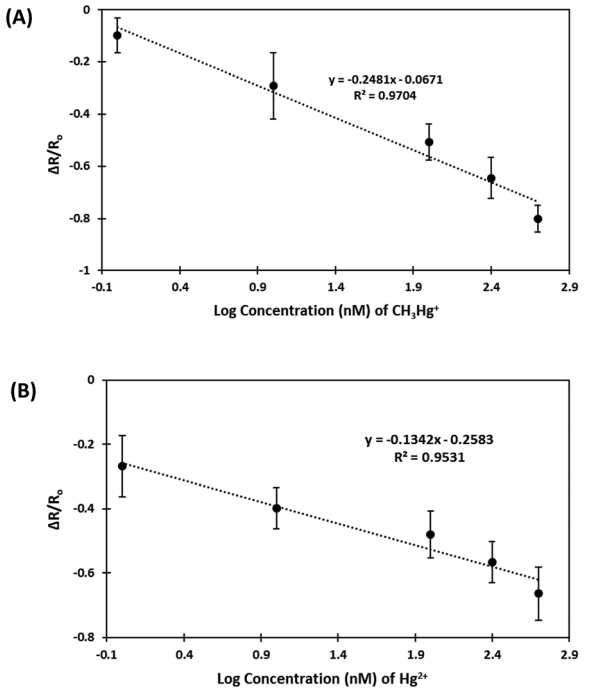

Fig. 3 Calibration curve for detection of (A) CH_3Hg^+ and (B) Hg^{2+} in simulated human saliva. Each data point is an average of measurements from 7 (in the case of CH_3Hg^+) and 6 (in the case of Hg^{2+}) independent sensors and error bars represent ±1 standard deviation.

specific binding of mucin on gold. A negative control experiment was performed to test the response of DNA-functionalized biosensor to simulated human saliva in the absence of Hg^{2+} ions. As shown in Fig. S3,† in the absence of Hg^{2+} ions, the response to simulated saliva was <1%, which confirms the absence of any non-specific binding of proteins. As shown in Fig. 3, for simulated saliva spiked with Hg^{2+} ion concentrations varying from 1 nM to 500 nM, a linear response with a regression equation of $y = -0.1342x - 0.2583$ ($R^2 = 0.9531$) and good reproducibility (evidenced by low standard deviation) was obtained. The sensitivity of 13.42% per log (nM) of Hg^{2+} was 40% lower than the sensitivity of 21.64% per log (nM) of Hg^{2+} in buffer solution. Similarly for saliva samples spiked with CH_3Hg^+ ion concentrations varying from 1 nM to 500 nM a linear regression equation of $y = -0.2481x - 0.0671$ ($R^2 = 0.9704$) was obtained. Further, the biosensors had good reproducibility. The sensitivity of 24.81% per log (nM) of CH_3Hg^+ was comparable to the sensitivity of 28.34% per log (nM) of CH_3Hg^+ in buffer solution but higher than for Hg^{2+} in saliva. These results demonstrate the high selectivity, specificity and reproducibility of the proposed biosensor which allows for detection of Hg^{2+} and CH_3Hg^+ in a complex matrix without any sample pretreatment.

Conclusions

We have demonstrated a sensitive, selective and label-free SWNT-based chemiresistive biosensor for the facile detection of divalent mercuric (Hg^{2+}) and monomethyl mercury (CH_3Hg^+) ions in simulated saliva. The device utilizes the novel structure-switching mechanism of polyT oligonucleotides upon specific interactions with mercury ions to induce dehybridization of polyA oligonucleotides from the preformed polyT:polyA duplexes at the SWNT surface. This structure-switch causes a measureable change in device resistance which is used to quantify the mercury concentration. Overall, the biosensor exhibited good selectivity and sensitivity for CH_3Hg^+ and Hg^{2+} ions in simulated saliva with a linear detection range of 1 nM to 500 nM and a sensitivity of 24.81% and 15.68% per log (nM) of CH_3Hg^+ and Hg^{2+}, respectively. This detection strategy is the first report for the quantification of Hg ions in saliva without the use of labels while eliminating complex assay procedures. Therefore, the biosensor reported here provides a viable tool for mercury detection in biological samples.

Acknowledgements

We acknowledge the financial support of NIH grant 1R43ES023707-01.

References

1 F. Zahir, S. J. Rizwi, S. K. Haq and R. H. Khan, *Environ. Toxicol. Pharmacol.*, 2005, **20**, 351–360.
2 F. J. Dieguez-Acuña, W. W. Polk, M. E. Ellis, P. L. Simmonds, J. V. Kushleika and J. S. Woods, *Toxicol. Sci.*, 2004, **82**, 114–123.
3 J. Dolbec, D. Mergler, C. J. S. Passos, S. S. De Morais and J. Lebel, *Int. Arch. Occup. Environ. Health*, 2000, **73**, 195–203.
4 P. B. Tchounwou, W. K. Ayensu, N. Ninashvili and D. Sutton, *Environ. Toxicol.*, 2003, **18**, 149–175.
5 L. G. Dales, *Am. J. Med.*, 1972, **53**, 219–232.
6 N. E. Selin, *Annu. Rev. Environ. Resour.*, 2009, **34**, 43.
7 D. W. Boening, *Chemosphere*, 2000, **40**, 1335–1351.
8 M. Harada, *Teratology*, 1978, **18**, 285–288.
9 C. Cox, D. Marsh, G. Myers and T. Clarkson, *Neurotoxicology*, 1994, **16**, 727–730.
10 H. Kodaira, K. Ohno, N. Fukase, M. Kuroda, S. Adachi, M. Kikuchi and Y. Asada, *J. Oral Sci.*, 2013, **55**, 161–165.
11 P. D. Pigatto, *J. Hazard. Mater.*, 2010, **179**, 1166–1167.
12 V. A. Lemos and L. O. dos Santos, *Food Chem.*, 2014, **149**, 203–207.
13 C. Fernandez, A. C. Conceição, R. Rial-Otero, C. Vaz and J. L. Capelo, *Anal. Chem.*, 2006, **78**, 2494–2499.
14 Y. Cai, *TrAC, Trends Analyt. Chem.*, 2000, **19**, 62–66.
15 A. G. de Torres, J. M. C. Pavón and E. R. Castellon, *J. Anal. At. Spectrom.*, 1998, **13**, 243–248.
16 W. Yantasee, Y. Lin, K. Hongsirikarn, G. E. Fryxell, R. Addleman and C. Timchalk, *Environ. Health Perspect.*, 2007, 1683–1690.
17 Y. Zhou, L. Tang, G. Zeng, C. Zhang, Y. Zhang and X. Xie, *Sens. Actuators, B*, 2016, **223**, 280–294.
18 S. K. Vashist, D. Zheng, K. Al-Rubeaan, J. H. Luong and F. S. Sheu, *Biotechnol. Adv.*, 2011, **29**, 169–188.
19 T. Sarkar, Y. Gao and A. Mulchandani, *Appl. Biochem. Biotechnol.*, 2013, **170**, 1011–1025.
20 J. L. Gong, T. Sarkar, S. Badhulika and A. Mulchandani, *Appl. Phys. Lett.*, 2013, **102**, 013701.
21 T. Li, S. Dong and E. Wang, *Anal. Chem.*, 2009, **81**, 2144–2149.
22 Y. Tanaka, S. Oda, H. Yamaguchi, Y. Kondo, C. Kojima and A. Ono, *J. Am. Chem. Soc.*, 2007, **129**, 244–245.
23 C. Tlili, L. N. Cella, N. V. Myung, V. Shetty and A. Mulchandani, *Analyst*, 2010, **135**, 2637–2642.
24 P. Ramnani, Y. Gao, M. Ozsoz and A. Mulchandani, *Anal. Chem.*, 2013, **85**, 8061–8064.
25 X. Tang, S. Bansaruntip, N. Nakayama, E. Yenilmez, Y. L. Chang and Q. Wang, *Nano Lett.*, 2006, **6**, 1632–1636.
26 D. T. Wong, *J. Calif. Dent. Assoc.*, 2006, **34**, 283.
27 Z. Feldötö, T. Pettersson and A. Dedinaite, *Langmuir*, 2008, **24**, 3348–3357.